Neurosci. Bull. June, 2019, 35(3):378–388
https://doi.org/10.1007/s12264-019-00362-z

www.neurosci.cn
www.springer.com/12264

METHOD

Rapid and Sparse Labeling of Neurons Based on the Mutant Virus-Like Particle of Semliki Forest Virus

Fan Jia[1,2,3] · Xutao Zhu[2,3] · Pei Lv[2] · Liang Hu[2] · Qing Liu[1,2] · Sen Jin[3] · Fuqiang Xu[1,2,3,4]

Received: 21 August 2018 / Accepted: 23 October 2018 / Published online: 19 March 2019

Abstract Sparse labeling of neurons contributes to uncovering their morphology, and rapid expression of a fluorescent protein reduces the experiment range. To achieve the goal of rapid and sparse labeling of neurons *in vivo*, we established a rapid method for depicting the fine structure of neurons at 24 h post-infection based on a mutant virus-like particle of Semliki Forest virus. Approximately 0.014 fluorescent focus-forming units of the mutant virus-like particle transferred enhanced green fluorescent protein into neurons *in vivo*, and its affinity for neurons *in vivo* was stronger than for neurons *in vitro* and BHK21 (baby hamster kidney) cells. Collectively, the mutant virus-like particle provides a robust and convenient way to reveal the fine structure of neurons and is expected to be a helper virus for combining with other tools to determine their connectivity. Our work adds a new tool to the approaches for rapid and sparse labeling of neurons *in vivo*.

Keywords Semliki Forest virus · Mutant virus-like particle · Rapid labeling · Sparse labeling · Neuronal morphology

Introduction

A single neuron can project long-range from one region to other regions in the brain, which receives orders and sends information to execute different tasks [1–3]. The morphology and connectivity of neurons are important foundations of neuronal function. A tool for sparse labeling of neurons is a prerequisite to map their morphology, and this can contribute to elucidating their working mechanisms and discovering new functions. To achieve this goal, several labeling technologies have been developed, such as transgenic animals [4–7] and virus-based approaches [8–11]. These tools have clearly promoted the development of neuroscience [12–16]. However, animal-based methods are time-consuming and labor-intensive. Adeno-associated virus (AAV)-based tools are convenient approaches, but AAV can only hold < 4.5 kb of a foreign gene and needs a long time for protein expression [17]. Lentivirus also needs a long time for protein expression [18, 19]. Therefore, new tools with the properties of easy preparation, less time for protein expression, and a high cloning capacity are still needed in the neuroscience community.

To achieve these aims, it has been found that the mutant virus-like particle (VLP) of Semliki Forest virus (SFV)

Fan Jia and Xutao Zhu have contributed equally to this work.

Electronic supplementary material The online version of this article (https://doi.org/10.1007/s12264-019-00362-z) contains supplementary material, which is available to authorized users.

✉ Fan Jia
jiafan@wipm.ac.cn

✉ Fuqiang Xu
fuqiang.xu@wipm.ac.cn

1 State Key Laboratory of Magnetic Resonance and Atomic and Molecular Physics, Key Laboratory of Magnetic Resonance in Biological Systems, Wuhan Institute of Physics and Mathematics, Chinese Academy of Sciences, Wuhan 430071, China

2 Brain Research Center, Wuhan Institute of Physics and Mathematics, Chinese Academy of Sciences, Wuhan 430071, China

3 University of the Chinese Academy of Sciences, Beijing 100049, China

4 Center for Excellence in Brain Science and Intelligence Technology, Chinese Academy of Sciences, Shanghai 200031, China

might be a candidate. The SFV is a positive-strand RNA virus, which belongs to the Alphavirus genus of the Togaviridae family. SFV can infect neurons and cause encephalitis [20]. The vectors based on SFV, such as VLP [21, 22], have been developed to rapidly express foreign genes at high levels *in vitro* and *in vivo* [22–28]. In addition, the insertion capacity of the vector is up to 6.5 kb [26].

Here, we found that mutant VLP rapidly and sparsely labeled neurons *in vivo*, and visualized the fine structure of neurons in a sparse manner at 24 h post-infection based on the virus. Our work adds a new tool to the approaches for rapid and sparse labeling of neurons *in vivo*.

Materials and Methods

All procedures in this study were approved by the Animal Care and Use Committee at the Wuhan Institute of Physics and Mathematics, Chinese Academy of Sciences. All the experiments with viruses were performed in a Biosafety Level 2 laboratory and animal facilities.

Construction of the SFV-Enhanced Green Fluorescent Protein (EGFP) Replicon

To construct a clone of the SFV-EGFP replicon, an SFV4 replicon (kindly donated by Dr. Markus U. Ehrengruber, Department of Biology, Kantonsschule Hohe Promenade, Zurich, Switzerland) was used for engineering. The EGFP gene was amplified with the primer pairs 5'-CACAGAAT TCTGATTGGATCCACCATGGTGAGCAAGGGCGAG-GAG-3′ and 5′-GGATCGACTAGTGAACTCGAGTTA CTTGTACAGCTCGTCCATGCC-3′ and inserted into the replicon with BamHI and XhoI using In-Fusion HD Cloning kits (Takara), and the plasmid was verified by DNA sequencing.

Virus Production

The SFV-EGFP replicon and mutant helper RNAs were separately transcribed *in vitro* from the NruI and SpeI linearized cDNA plasmids using an SP6 mMACHINE kit (Ambion) according to the manufacturer's specifications. Then the RNAs were co-transfected into BHK21 (baby hamster kidney) cells using DMRIE-C reagent (Invitrogen). Briefly, 10 μL DMRIE-C was added to a tube containing 1 mL Opti-MEM I medium, then 10 μg of SFV replicon RNA and 10 μg of helper RNA were added to the tube and immediately transfected into 8×10^5 BHK-21 cells in 6-well plates.

Cells were washed three times using 1 mL Dulbecco's modified Eagle's medium (DMEM) with 2% fetal bovine serum (FBS) at 4 h post-transfection (hpt), then 1 mL medium (DMEM with 2% FBS) was added to the well and cells cultured in 5% CO_2 at 37 °C, and the supernatants were collected every 24 h until 4 days post-transfection. The culture medium containing the virus was filtered using a 0.22 μm filter and divided into two parts. One part was aliquoted and the other part was treated with α-chymotrypsin (final concentration 500 μg/mL) for 25 min at 37 °C, and aprotinin (final concentration 250 μg/mL) was added to stop the reaction. The virus was then aliquoted, titered, and stored at –80 °C.

SFV VLP Infects Neurons *In Vivo*

All procedures were approved by the Animal Care and Use Committees at the Wuhan Institute of Physics and Mathematics, Chinese Academy of Sciences. All the experiments with viruses were performed in a Biosafety Level 2 laboratory and animal facility. Eight-week-old male C57BL/6 mice (20 g–25 g) were used for virus injection. Animals were anesthetized with chloral hydrate (400 mg/kg), and placed in a stereotaxic apparatus (68030, 68025; RWD Life Sciences Inc., San Diego, CA). The skull above the targeted areas was thinned with a dental drill (90+102; STRONG, Guangdong, China) and removed carefully. Microinjections were made through a 10 μL syringe (Hamilton, Reno, NV) connected to a glass micropipette with 10 μm–15 μm diameter tip. The indicated volume of virus was stereotaxically microinjected into the target region. The micropipette was left in place for 10 min following injection to minimize diffusion. After the indicated times, mice were deeply anesthetized with an overdose of chloral hydrate and transcardially perfused with 0.9% saline followed by 4% paraformaldehyde. The brains were removed and post-fixed overnight in 4% paraformaldehyde before being cut into 30 μm sections which were stained with DAPI and imaged using a TCS SP8 confocal microscope (Leica).

Determining the Entry Site of SFV VLP Infecting Neurons

A microfluidic chamber was prepared as described in a previous study [29]. Briefly, a microfluidic device was bonded to a poly-D-lysine-coated glass coverslip to form the chamber. Dissociated neurons from embryonic mouse cortex (E16) were prepared as described previously. Approximately 300,000 cells were plated into one well of the chamber, designated the somal part. Neuronal axons extended along the microgroove to the axonal part within 2 weeks.

To analyze the soma-mediated infection of a neuron, the SFV VLP was loaded into the somal part and the EGFP

signals were detected at the indicated time points. To determine the axon-mediated infection of a neuron, the SFV VLP was loaded into the axonal part and the EGFP signal located in the somal part was imaged at the indicated time points.

Immunohistochemical Assays *In Vitro* and *In Vivo*

To stain neurons *in vitro*, the neuron cultures and staining procedures were as in a previous study [28]. Briefly, neurons were isolated and cultured in medium (Neurobasal medium, penicillin-streptomycin-glutamine, and B27 supplement) on 24-well plates in 5% CO_2 at 37 °C. Infected neurons were fixed in 4% paraformaldehyde at room temperature for 30 mins. Then the cells were incubated with Cy3-conjugated rabbit antibody against NeuN (1:200; ABN78C3 Merck Millipore,) and visualized using a fluorescence microscope (IX73, Olympus).

To stain neurons *in vivo*, the protocol was as in a previous study [28]. Briefly, the post-fixed brain was cut into 40-μm coronal sections and the fixed sections were immunostained with the Cy3-conjugated rabbit antibody against NeuN (1:100; ABN78C3; Merck Millipore).

To stain Purkinje cells, fixed sagittal sections 80 μm thick were immunostained with a mouse monoclonal antibody against calbindin-D28k (Proteintech) and amplified with a Cy3-conjugated anti-mouse secondary antibody (Merck). Imaging was performed using a TCS SP8 confocal microscope (Leica).

Results

Mutant SFV VLP Infects Neurons *In Vitro* and *In Vivo*

Virus-based tools are used to deliver genes into cells *via* the interaction of a virus envelope protein with receptors on the cell surface [30]. A previous study has shown that a three amino-acid mutation in the SFV E3 protein fully blocks the interaction and results in the loss of infectivity [22]. Here, the mutant VLP of SFV with the EGFP reporter was prepared by co-transfection of the replicon and mutant helper RNAs into BHK21 cells [21, 22] (Fig. 1A). EGFP signals were detected at 6 hpt, and were enhanced with time (Fig. 1B). The supernatant, containing mutant SFV VLP, was collected at 48 hpt and loaded into wells in which BHK21 cells were being cultured. Only a few EGFP-positive BHK21 cells were found (Fig. 1C). This result is not consistent with previous reports, which showed that mutant VLP is non-infectious [22]. The current result indicates that the three amino-acid mutation in SFV E3 does not fully eliminate the ability of the virus to enter cells, but significantly reduce its infection efficiency. When the mutant VLP was treated with α-chymotrypsin to produce wild-type SFV VLP, the infection efficiency significantly increased (Fig. 1C). The α-chymotrypsin was toxic to neurons *in vitro* and *in vivo* (data not shown). The amount of VLP increased from 6 h to 48 h (Fig. 1B), with a peak value of $\sim 10^4$ FFU (fluorescent-focus forming units)/mL for the mutant and $\sim 10^7$ FFU/mL for the wild-type (Fig. 1D). We then investigated the ability of mutant VLP to infect neurons *in vitro* and *in vivo*. The mutant VLP (2.3×10^2 FFU, tested on BHK21 cells) was loaded into plate wells containing neurons. The EGFP signals were imaged at 24 hpi and co-localized with the neuronal marker NeuN (Fig. 1E), which confirmed that the mutant VLP did infect neurons *in vitro*. In addition, the wild-type VLP (4×10^4 FFU) also infected neurons *in vitro* (Fig. 1E), consistent with previous reports [28, 31, 32]. Therefore, we speculated that these two viruses can infect neurons *in vivo*. Equal volumes of mutant and wild-type VLP were then separately injected into the ventral posteromedial nucleus of the thalamus (VPM) of the mouse brain at the following coordinates: −1.70 mm posterior to bregma, −1.40 mm lateral to the midline, and −3.65 dorsoventral relative to bregma, and the EGFP signals were imaged at 24 hpi. Interestingly, the wild-type VLP was found in a large number of labeled neurons, while the mutant virus was transduced into fewer neurons (Fig. 1F). The EGFP signals at 24 hpi were co-localized with the neuronal marker NeuN (Fig. 1G). These results demonstrated that the mutant VLP is able to sparsely label neurons *in vivo*.

Mutant SFV VLP Infects Neurons Anterogradely

The entry site of SFV VLP was determined using the microfluidic chamber, which is a platform for testing the entry site when a virus infects a neuron [29]. Neurons were cultured in the somal parts of the chamber and axons extended into the axonal parts of the chamber within 2 weeks (Fig. 2A). The mutant VLP (23 FFU) was loaded into either the somal or the axonal chamber, and EGFP signals were detected in the axonal and somal chambers at 24 hpi after the virus was added to the somal chamber, while no EGFP signal was detected when the virus was added to the axonal chamber (data not shown). These results indicate that the mutant virus is able to enter neurons using a non-axonal pathway. However, these results cannot exclude the possibility that the mutant virus enters neurons through axon terminals when a high titer of virus is applied. Therefore, in order to adequately estimate the characteristics of the viral infection of neurons, the wild-type VLP (5×10^5 FFU) was added to the somal chamber, and EGFP signals were evident in the axonal and somal chambers at 24 hpi (Fig. 2A). When the wild-type

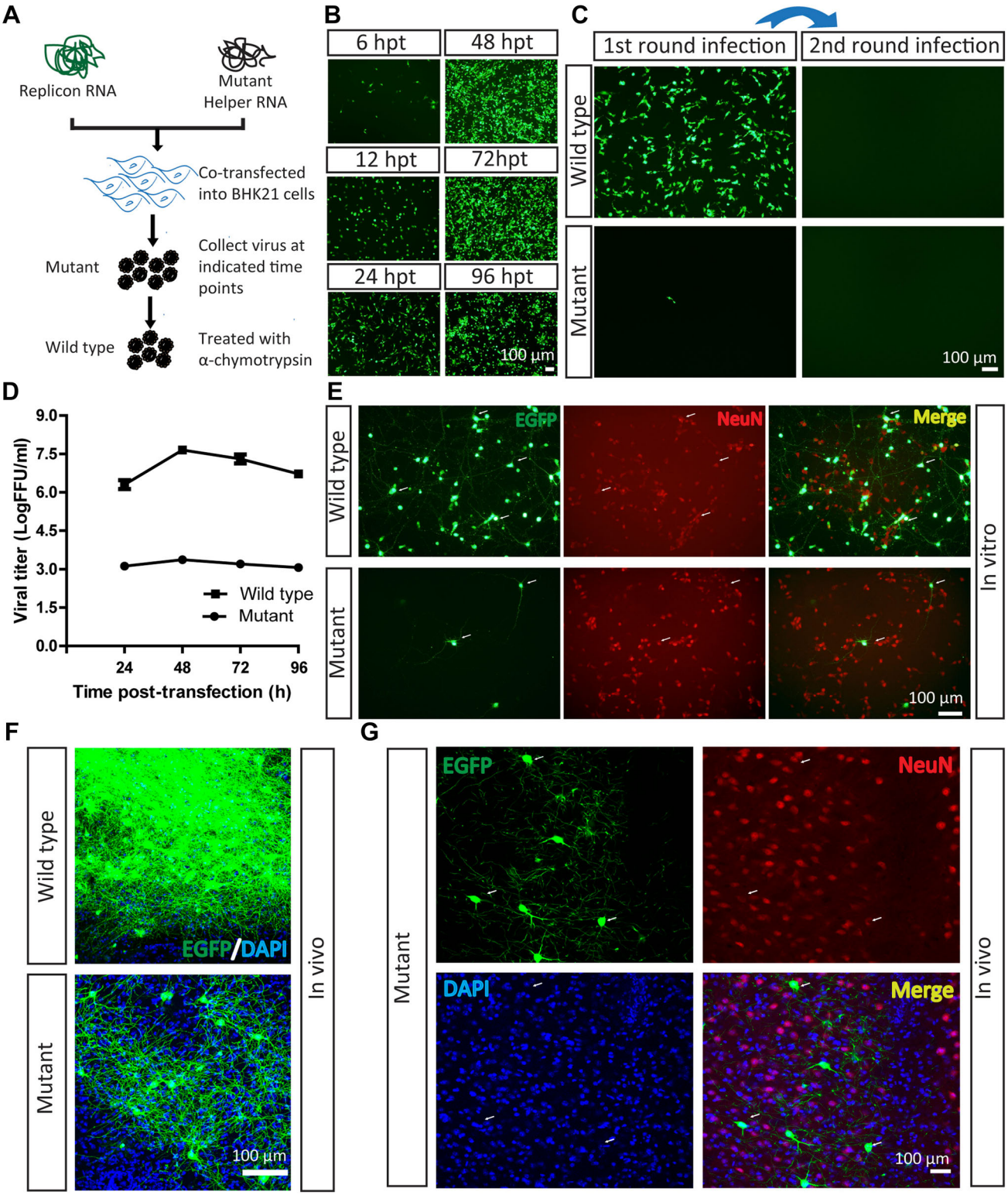
A
Replicon RNA
Mutant Helper RNA
Co-transfected into BHK21 cells
Collect virus at indicated time points
Mutant
Wild type
Treated with α-chymotrypsin
B
6 hpt
48 hpt
12 hpt
72hpt
24 hpt
96 hpt
100 μm
C
1st round infection
2nd round infection
Wild type
Mutant
100 μm
D
Viral titer (LogFFU/ml)
9.0
7.5
6.0
4.5
3.0
1.5
0.0
24
48
72
96
Time post-transfection (h)
Wild type
Mutant
E
Wild type
Mutant
EGFP
NeuN
Merge
100 μm
In vitro
F
Wild type
Mutant
EGFP/DAPI
100 μm
In vivo
G
Mutant
EGFP
NeuN
DAPI
Merge
100 μm
In vivo

◀**Fig. 1** Mutant SFV VLP infects neurons *in vitro* and *in vivo*. **A** Work flow for preparation of SFV VLP. **B** Virus production. Replicon and mutant helper RNAs were co-transfected into BHK21 cells. The EGFP signals were first detected at 6 hpi, and became enhanced with time. **C** Mutant SFV VLP had lower entry efficiency with a single round of infection. The mutant SFV VLP was treated with α-chymotrypsin to restore infectivity and prepare the wild-type virus, then it was loaded into a BHK21 well and EGFP was observed at 24 hpi. Fresh BHK21 cells were infected with culture medium collected from cells after the first infection at 24 hpi, but no EGFP signal was detected. In addition, the mutant virus also infected BHK21 cells, and fresh BHK21 cells were infected by culture medium collected from cells after the first infection at 24 hpi, but no EGFP signal was detected. **D** Growth curves of the mutant and wild-type viruses. The mutant and wild-type virus (treated with α-chymotrypsin) were titered in BHK21 cells. **E** Wild-type and mutant SFV VLP delivered EGFP into neurons *in vitro*. Cultured neurons were separately infected with mutant and wild-type viruses. After 24 hpi, the EGFP signals were imaged. The neurons were stained with antibody conjugated to Cy3 against neuron-specific protein NeuN. **F** Wild-type (100 nL, 6×10^7 FFU/mL) and mutant viruses (100 nL, 1.2×10^4 FFU/mL) were each injected into the VPM region of mouse brain. After 24 hpi, brain sections were prepared. The wild-type virus labeled many neurons and the mutant virus labeled a few neurons. These images are representative of 15 sections (n = 3 mice). **G** Mutant virus was injected into the VPM region. After 24 hpi, sections were prepared. The EGFP signals co-localized with signals of the neural marker NeuN (arrows). These images are representative of 15 sections (n = 3 mice).

virus was added to the axonal chamber, no EGFP signals were found in the axonal and somal chambers, even using a higher titer of virus (data not shown). These results demonstrate that SFV VLP enters neurons non-axonally and is anterogradely transported *in vitro*. Furthermore, we tested the entry site of the virus on neurons *in vivo*. When the wild-type VLP was injected into the VPM, it locally infected neurons in the injection site (Fig. 2B). Rare EGFP signals were detected in the contralateral subiculum when the virus was injected into the subiculum (data not shown). In addition, when the mutant VLP was injected into the VPM, EGFP signals were observed in the VPM region and primary sensory cortex at 24 hpi (Fig. 2C). These results indicated that SFV VLP is anterogradely transported, but with limited retrograde uptake, similar to the Sindbis virus that belongs to the same family [33].

Rapid and Sparse Labeling of Neurons by Mutant SFV VLP *In Vivo*

Based on the above data (Fig. 1F), we speculated that the mutant VLP may be a powerful tool for rapid and sparse labeling of neurons to display fine neuronal morphology. Thus, the cerebellar cortex was selected as a model region to test the ability of the mutant VLP to rapidly and sparsely label neurons *in vivo*. First, to characterize the time course of the mutant VLP labeling, mutant VLP (0.69 FFU) was injected into the third cerebellar lobule (3Cb) region at the following coordinates: 6.40 mm posterior to bregma, 0.5 mm lateral to the midline, 2.30 dorsoventral relative to bregma. Mice were sacrificed at 12 hpi, 24 hpi, 48 hpi, 72 hpi, and 96 hpi. EGFP signals were detected in the 3Cb at 12 hpi, and increased with time (Fig. 3). Each section containing the 3Cb had several EGFP-positive neurons, and the best time for clearly observing neuronal morphology was between 24 hpi and 48 hpi. The EGFP signals were clearly imaged and co-localized with the Purkinje cell marker calbindin-D28k (Fig. 4A). In sagittal sections (80 μm thick), the Purkinje cells were clearly labeled. The dendritic tree was apparent and the axon was long, with many branches (Fig. 4B and Supplementary Movie S1). Furthermore, the mutant SFV VLP also sparsely labeled hippocampal pyramidal neurons in the CA1 region [34] (Fig. 5A) and mossy cells in the dentate gyrus region [35–37] (Fig. 5B) based on the morphological characteristics of the neurons. Taken together, these results indicated that the mutant VLP is a candidate for rapid and sparse labeling of neurons *in vivo*.

Mutant SFV VLP Has Higher Infection Efficiency in Neurons *In Vivo*

When we analyzed the infection efficiency of mutant VLP in BHK21 cells and neurons, the mutant VLP (11.5 FFU, tested on BHK21 cells) infected and stained 120 ± 7.8 EGFP-positive neurons *in vitro* (Fig. 6A), and the mutant VLP at 0.115 FFU injected into the target region of mouse brain (– 1.70 from bregma) stained 8 ± 3.2 EGFP-positive neurons (Fig. 6A). These results showed that the infection efficiency in BHK21 cells was lower than in neurons *in vitro* and *in vivo*, and the infection efficiency in neurons *in vivo* was higher than *in vitro*. These results demonstrate that 0.096 FFU and ∼0.014 FFU of the mutant VLP can infect a neuron *in vitro* and *in vivo*, respectively. In addition, we found that the viral titer differed among these cells. The order of the titer was: neurons *in vivo* > neurons *in vitro* > BHK21 cells (Fig. 6B). These results also indicated that the infection efficiency is different in these cells. We speculated that the difference between neurons *in vitro* and *in vivo* was due to (i) interactions between glial cells and neurons [38, 39], and (ii) the micro-environment around neurons [40]. Previous reports have shown that neurons co-cultured with glial cells display a significantly increased transfection efficiency [38]. In addition, the discrepancy between BHK21 cells and neurons might have been due to (i) BHK21 cells are larger than neurons, so each BHK21 cell needs more viral genome when a virus infects it, and (ii) many alphavirus receptors have been identified, such as the high-affinity laminin receptor [41], α1β1 integrin [42], heparan sulfate [43], DC-SIGN and

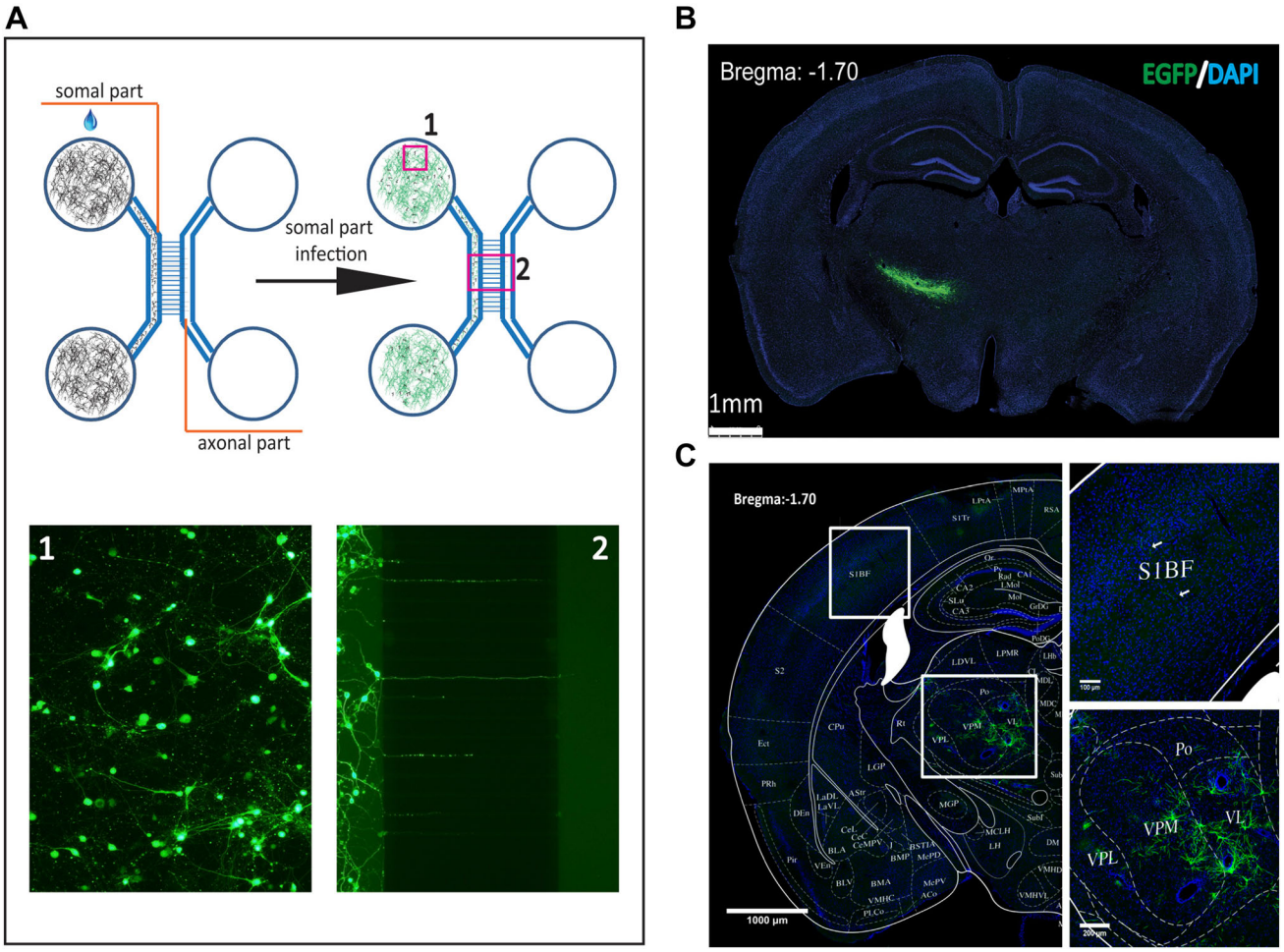

Fig. 2 Entry site of SFV VLP infection of neurons. **A** The microfluidic chamber was made of polydimethylsiloxane (Dow Corning, Midland, MI) and used to determine the efficiency of anterograde axonal spread. Neurons were plated in the somal part (1), and axons extended to the axonal part (2) along the microgrooves at 10 days post-culture. To test the non-axonal entry site, the wild-type virus was loaded into the somal part and the EGFP signal was imaged at 24 hpi. To test the axonal entry site, the wild-type virus was loaded into the axonal part and the EGFP signal was detected at 24 hpi (data not shown). **B, C** Entry site of SFV VLP infection of neurons *in vivo*. Wild-type (**B**) and mutant (**C**) SFV VLP were injected into the VPM region, then sections were prepared at 24 hpi and the EGFP signal was imaged. These images are representative of 15 sections ($n = 3$ mice). VPM, ventral posteromedial thalamic nucleus; S1BF, primary somatosensory cortex, barrel field.

L-SIGN [44], and Mxra8 [45], so the efficiency of receptors that mediate the entry of virus into cells might be different. Based on the data, we proposed models for VLP infection of BHK21 cells and neurons *in vitro* and *in vivo* (Fig. 6C). However, the precise mechanism of infection in different cells needs to be determined in future.

Discussion

Mutant E3 Does Not Fully Eliminate Infectivity, but Significantly Reduces Infection Efficiency

Twenty years ago, Liljestrom and Garoff developed the replication-deficient SFV vector for protein expression *in vitro* and *in vivo* [21]. To enhance the safety of the tool, three amino-acids in SFV E3 were mutated to eliminate its infectivity [22]. The mutant SFV VLP has to be treated with α-chymotrypsin to restore the infectivity [22]. However, in this study, we found that the three amino-acid mutation did not fully eliminate the infectivity of SFV, rather it significantly reduced the infection rate (Fig. 1). Furthermore, we found that the mutant SFV VLP could be used for rapid and sparse labeling of neurons *in vivo* (Figs. 4 and 5). Therefore, the mutant SFV VLP is a convenient tool for preparation without treatment with more reagents (such as α-chymotrypsin). In addition, wild-type SFV VLP (treated with α-chymotrypsin) also rapidly and sparsely labeled neurons *in vivo*, but their morphology

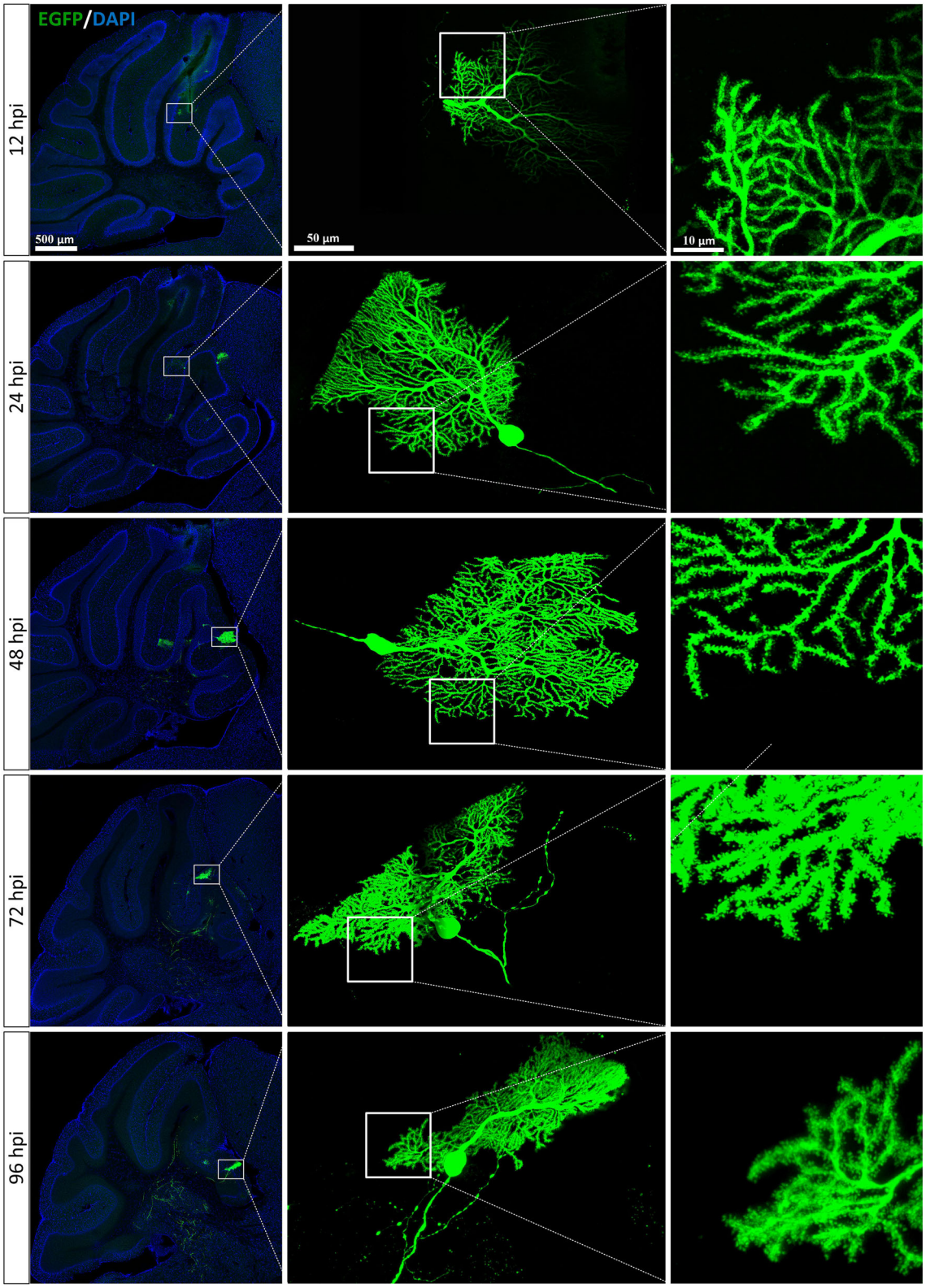

Fig. 3 Time course of SFV VLP infection of neurons. The mutant virus was injected into the 3Cb region of mouse brain and sections were prepared at 12 hpi, 24 hpi, 48 hpi, 72 hpi, and 96 hpi). These images are representative of 15 sections at the indicated time points (n = 3 mice at each time point).

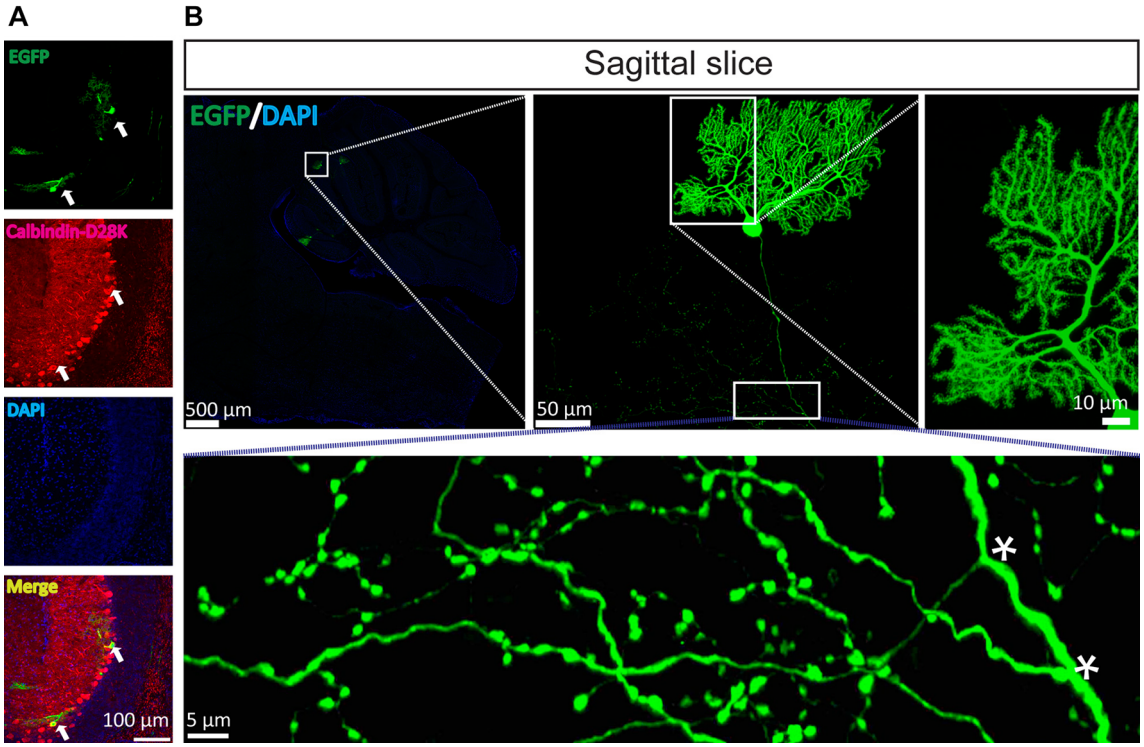

Fig. 4 Mutant SFV VLP rapidly and sparsely labels Purkinje neurons *in vivo*. To sparsely label Purkinje cells, the mutant virus was injected into the third cerebellar lobule (3Cb) region. The mice were sacrificed at 24 hpi and sagittal and coronal sections were prepared. **A** The EGFP signals were co-localized with the Purkinje cell marker calbindin-D28k (arrows). **B** The fine structure of the Purkinje cells was apparent, including the dendritic tree, long axon, and axonal branches (asterisks). These images are representative of 15 sections (n = 3 mice).

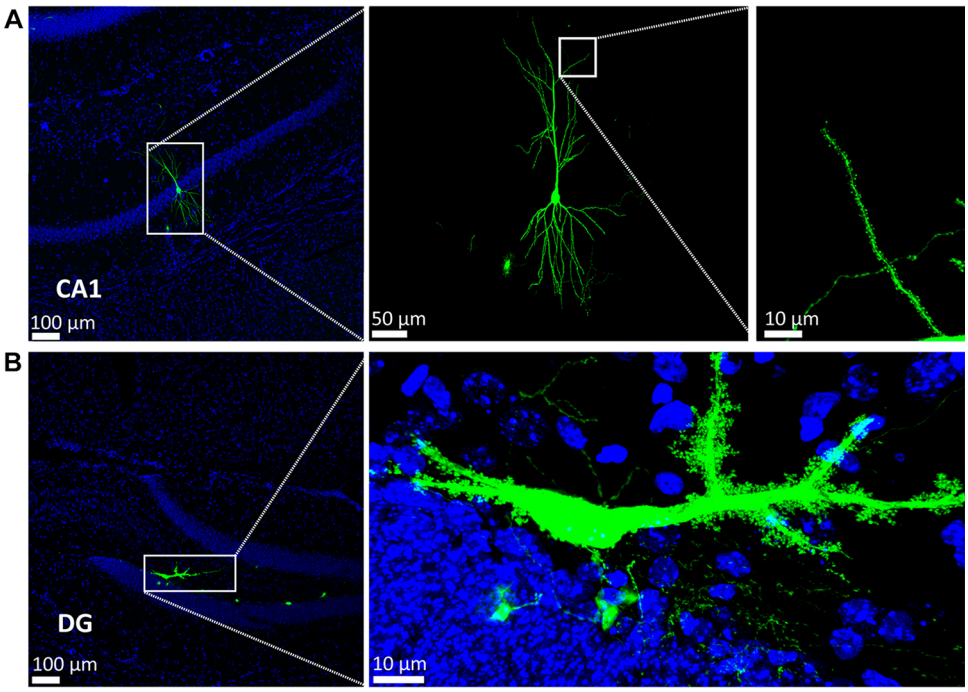

Fig. 5 Mutant SFV VLP rapidly and sparsely labels other types of neurons *in vivo*. To test whether the mutant virus sparsely labels other neurons, the virus was injected into the CA1 field of the hippocampus (CA1, **A**) and dentate gyrus (DG, **B**). After 24 hpi, sections were prepared and the EGFP signals were imaged. Hippocampal pyramidal neurons (**A**) and mossy cells (**B**) were labeled.

A

Virus name	Infectious virus applied (FFU, tested in BHK21 cells)	The number of EGFP-positive neurons
Mutant	11.5	120 ± 7.8 (*in vitro*)
	0.115	>8 ± 3.2 (*in vivo*)

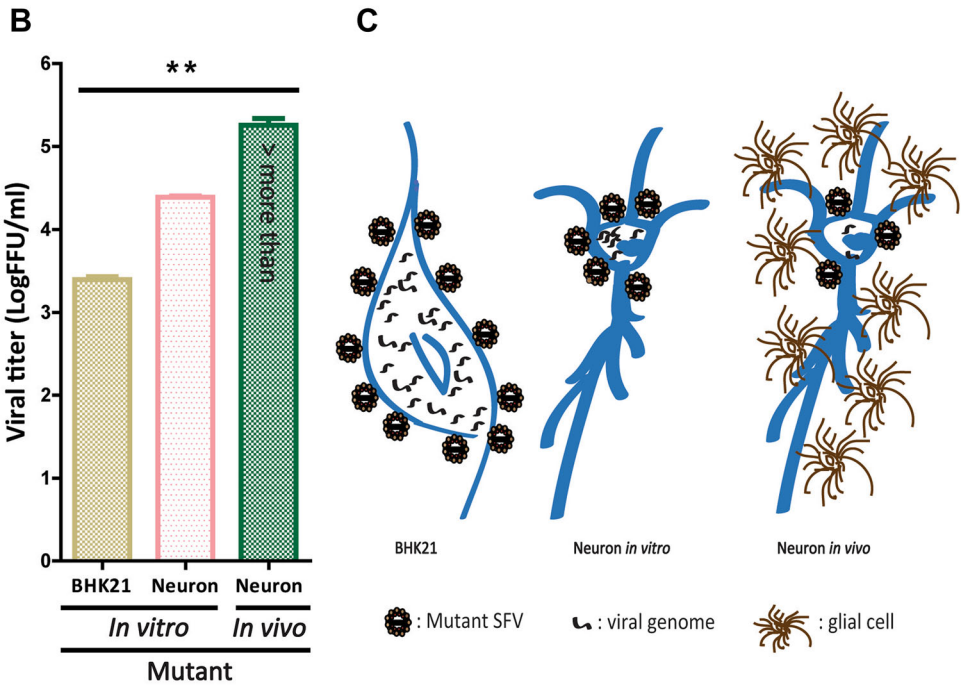

Fig. 6 Mutant SFV VLP enters BHK21 cells and neurons *in vitro* and neurons *in vivo* with different infection efficiency. **A** Three mice were tested and 15 sections were analyzed to determine the infection efficiency of the mutant virus on neurons *in vivo*. **B** Differences in infection efficiency of the mutant virus in different cells ($n = 3$; $^{**}P < 0.01$, one-way ANOVA; error bars indicate standard error of the mean from the three independent experiments). **C** Models of mutant virus infection of BHK21 cells, neurons *in vitro*, and neurons *in vivo*.

was less intact due to the toxicity of α-chymotrypsin (data not shown).

Mutant SFV VLP as a Tool for Rapid and Sparse Labeling of Neurons *In Vivo*

To sparsely label neurons *in vivo*, several methods have been developed. Feng *et al.* constructed a transgenic mouse in which different fluorescent proteins were selectively expressed in wild-type neurons [46]. Badea *et al.* generated a transgenic mouse to directly and sparsely label neurons using a CreER(T)/loxP strategy [6]. Zhang *et al.* and Barski *et al.* prepared Pcp2-cre mice to specifically express Cre recombinase in Purkinje cells, and these were crossed with transgenic mice containing a Cre-activated cassette to establish transgenic lines for analyzing the function and morphology of neurons [47–50]. However, animal-based approaches are time-consuming and labor-intensive. Virus-based methods are convenient and are complementary to the use of transgenic animals.

Gibson and Ma developed a method for sparsely labeling neurons by controlling the titer of AAV [8, 9]. In addition, a mixture of AAV expressing Cre recombinase and Cre-dependent AAV sparsely labels neurons *in vivo* [51]. Lentivirus can also be used for the sparse mapping of neurons *in vivo* [52]. Combination of Pcp2-cre mice with Cre-dependent virus also specifically expresses target protein in Purkinje cells [47, 48]. AAV has an insertion capacity < 4.5 kb and usually needs > 21 days for protein expression *in vivo* [10, 17]. Lentivirus has an insertion capacity up to 10 kb and usually needs > 7 days for protein expression *in vivo* [18, 53]. The mutant VLP rapidly and sparsely labeled neurons *in vivo* at 24 hpi (Figs. 4 and 5), and the insertion capacity is up to 6.5 kb [26]. In this study, we found that ~0.014 FFU of mutant VLP can infect a neuron *in vivo* (Fig. 3). Recombinant AAV and lentivirus

usually need a higher titer of the virus to infect a neuron [26]. The discrepancy is that the SFV contains a replicase, while recombinant AAV and lentivirus do not. Therefore, the preparation protocol for the mutant SFV is convenient because it is not necessary to prepare high titer of the virus. AAV and lentivirus can express protein using a cell-type-specific promoter. The current version of the SFV-based tool cannot express protein using a cell-type-specific promoter because the genome of SFV is RNA.

Taken together, the mutant SFV VLP can serve as a tool to rapidly and sparsely label neurons for morphological studies and neural circuit tracing in combination with trans-synaptic tools.

Acknowledgements We are grateful to Dr. Markus U. Ehrengruber (Department of Biology, Kantonsschule Hohe Promenade, Zurich, Switzerland) for providing the SFV replicon and helper cDNA clones. This work was supported by the National Natural Science Foundation of China (31771197,31830035 and 91732304), the National Basic Research Development Program (973 Program) of China (2015CB755600), the Strategic Priority Research Program (B), Chinese Academy of Sciences, China (XDBS01030200), and the Major Research Plan of the National Natural Science Foundation of China (91632303).

Conflict of interest All authors declare that they have no conflict of interest.

References

1. Apps R, Garwicz M. Anatomical and physiological foundations of cerebellar information processing. Nat Rev Neurosci 2005, 6: 297–311.
2. Jefferis GS, Livet J. Sparse and combinatorial neuron labelling. Curr Opin Neurobiol 2012, 22: 101–110.
3. Carletti B, Williams IM, Leto K, Nakajima K, Magrassi L, Rossi F. Time constraints and positional cues in the developing cerebellum regulate Purkinje cell placement in the cortical architecture. Dev Biol 2008, 317: 147–160.
4. Lee T, Luo L. Mosaic analysis with a repressible cell marker for studies of gene function in neuronal morphogenesis. Neuron 1999, 22: 451–461.
5. Rotolo T, Smallwood PM, Williams J, Nathans J. Genetically-directed, cell type-specific sparse labeling for the analysis of neuronal morphology. PLoS One 2008, 3: e4099.
6. Badea TC, Hua ZL, Smallwood PM, Williams J, Rotolo T, Ye X, *et al.* New mouse lines for the analysis of neuronal morphology using CreER(T)/loxP-directed sparse labeling. PLoS One 2009, 4: e7859.
7. Potter CJ, Tasic B, Russler EV, Liang L, Luo L. The Q system: a repressible binary system for transgene expression, lineage tracing, and mosaic analysis. Cell 2010, 141: 536–548.
8. Gibson DA, Ma L. Mosaic analysis of gene function in postnatal mouse brain development by using virus-based Cre recombination. J Vis Exp 2011.
9. Gibson DA, Tymanskyj S, Yuan RC, Leung HC, Lefebvre JL, Sanes JR, *et al.* Dendrite self-avoidance requires cell-autonomous slit/robo signaling in cerebellar purkinje cells. Neuron 2014, 81: 1040–1056.
10. Bosch MK, Nerbonne JM, Ornitz DM. Dual transgene expression in murine cerebellar Purkinje neurons by viral transduction *in vivo*. PLoS One 2014, 9: e104062.
11. Goenawan H, Hirai H. Modulation of lentiviral vector tropism in cerebellar Purkinje cells *in vivo* by a lysosomal cysteine protease cathepsin K. J Neurovirol 2012, 18: 521–531.
12. Nassi JJ, Cepko CL, Born RT, Beier KT. Neuroanatomy goes viral! Front Neuroanat 2015, 9: 80.
13. Kim EJ, Jacobs MW, Ito-Cole T, Callaway EM. Improved monosynaptic neural circuit tracing using engineered rabies virus glycoproteins. Cell Rep 2016, 15: 692–699.
14. Lo L, Anderson DJ. A Cre-dependent, anterograde transsynaptic viral tracer for mapping output pathways of genetically marked neurons. Neuron 2011, 72: 938–950.
15. Smith BN, Banfield BW, Smeraski CA, Wilcox CL, Dudek FE, Enquist LW, *et al.* Pseudorabies virus expressing enhanced green fluorescent protein: A tool for *in vitro* electrophysiological analysis of transsynaptically labeled neurons in identified central nervous system circuits. Proc Natl Acad Sci USA 2000, 97: 9264–9269.
16. Osakada F, Mori T, Cetin AH, Marshel JH, Virgen B, Callaway EM. New rabies virus variants for monitoring and manipulating activity and gene expression in defined neural circuits. Neuron 2011, 71: 617–631.
17. Grieger JC, Samulski RJ. Packaging capacity of adeno-associated virus serotypes: impact of larger genomes on infectivity and postentry steps. J Virol 2005, 79: 9933–9944.
18. Takayama K, Torashima T, Horiuchi H, Hirai H. Purkinje-cell-preferential transduction by lentiviral vectors with the murine stem cell virus promoter. Neurosci Lett 2008, 443: 7–11.
19. Zhang F, Qian X, Qin C, Lin Y, Wu H, Chang L, *et al.* Phosphofructokinase-1 negatively regulates neurogenesis from neural stem cells. Neurosci Bull 2016, 32: 205–216.
20. Fazakerley JK. Pathogenesis of Semliki Forest virus encephalitis. J Neurovirol 2002, 8 Suppl 2: 66–74.
21. Liljestrom P, Garoff H. A new generation of animal cell expression vectors based on the Semliki Forest virus replicon. Biotechnology 1991, 9: 1356–1361.
22. Berglund P, Sjoberg M, Garoff H, Atkins GJ, Sheahan BJ, Liljestrom P. Semliki Forest virus expression system: production of conditionally infectious recombinant particles. Biotechnology 1993, 11: 916–920.
23. Andrell J, Tate CG. Overexpression of membrane proteins in mammalian cells for structural studies. Mol Membr Biol 2013, 30: 52–63.
24. Blasey HD, Lundstrom K, Tate S, Bernard AR. Recombinant protein production using the Semliki Forest Virus expression system. Cytotechnology 1997, 24: 65–72.
25. Ehrengruber MU, Lundstrom K, Schweitzer C, Heuss C, Schlesinger S, Gahwiler BH. Recombinant Semliki Forest virus and Sindbis virus efficiently infect neurons in hippocampal slice cultures. Proc Natl Acad Sci USA 1999, 96: 7041–7046.
26. Ehrengruber MU, Hennou S, Bueler H, Naim HY, Deglon N, Lundstrom K. Gene transfer into neurons from hippocampal slices: comparison of recombinant Semliki Forest virus, adenovirus, adeno-associated virus, lentivirus, and measles virus. Mol Cell Neurosci 2001, 17: 855–871.
27. Lundstrom K. Alphaviruses in gene therapy. Viruses 2015, 7: 2321–2333.
28. Jia F, Miao H, Zhu X, Xu F. Pseudo-typed Semliki Forest virus delivers EGFP into neurons. J Neurovirol 2017, 23: 205–215.
29. Liu WW, Goodhouse J, Jeon NL, Enquist LW. A microfluidic chamber for analysis of neuron-to-cell spread and axonal transport of an alpha-herpesvirus. PLoS One 2008, 3: e2382.

30. Casasnovas JM. Virus-receptor interactions and receptor-mediated virus entry into host cells. Subcell Biochem 2013, 68: 441–466.
31. Sato Y, Shiraishi Y, Furuichi T. Cell specificity and efficiency of the Semliki Forest virus vector- and adenovirus vector-mediated gene expression in mouse cerebellum. J Neurosci Methods 2004, 137: 111–121.
32. Lundstrom K, Abenavoli A, Malgaroli A, Ehrengruber MU. Novel Semliki Forest virus vectors with reduced cytotoxicity and temperature sensitivity for long-term enhancement of transgene expression. Mol Ther 2003, 7: 202–209.
33. Kebschull JM, Garcia da Silva P, Zador AM. A new defective helper RNA to produce recombinant Sindbis virus that infects neurons but does not propagate. Front Neuroanat 2016, 10: 56.
34. Beaudoin GM, 3rd, Lee SH, Singh D, Yuan Y, Ng YG, Reichardt LF, *et al.* Culturing pyramidal neurons from the early postnatal mouse hippocampus and cortex. Nat Protoc 2012, 7: 1741–1754.
35. GoodSmith D, Chen X, Wang C, Kim SH, Song H, Burgalossi A, *et al.* Spatial representations of granule cells and mossy cells of the dentate gyrus. Neuron 2017, 93: 677–690 e675.
36. Ribak CE, Seress L, Amaral DG. The development, ultrastructure and synaptic connections of the mossy cells of the dentate gyrus. J Neurocytol 1985, 14: 835–857.
37. Scharfman HE, Schwartzkroin PA. Electrophysiology of morphologically identified mossy cells of the dentate hilus recorded in guinea pig hippocampal slices. J Neurosci 1988, 8: 3812–3821.
38. Majumdar D, Gao Y, Li D, Webb DJ. Co-culture of neurons and glia in a novel microfluidic platform. J Neurosci Methods 2011, 196: 38–44.
39. Meyer K, Kaspar BK. Glia-neuron interactions in neurological diseases: testing non-cell autonomy in a dish. Brain Res 2017, 1656: 27–39.
40. Namba T, Funahashi Y, Nakamuta S, Xu C, Takano T, Kaibuchi K. Extracellular and intracellular signaling for neuronal polarity. Physiol Rev 2015, 95: 995–1024.
41. Wang KS, Kuhn RJ, Strauss EG, Ou S, Strauss JH. High-affinity laminin receptor is a receptor for Sindbis virus in mammalian cells. J Virol 1992, 66: 4992–5001.
42. La Linn M, Eble JA, Lubken C, Slade RW, Heino J, Davies J, *et al.* An arthritogenic alphavirus uses the alpha1beta1 integrin collagen receptor. Virology 2005, 336: 229–239.
43. Gardner CL, Ebel GD, Ryman KD, Klimstra WB. Heparan sulfate binding by natural eastern equine encephalitis viruses promotes neurovirulence. Proc Natl Acad Sci U S A 2011, 108: 16026–16031.
44. Klimstra WB, Nangle EM, Smith MS, Yurochko AD, Ryman KD. DC-SIGN and L-SIGN can act as attachment receptors for alphaviruses and distinguish between mosquito cell- and mammalian cell-derived viruses. J Virol 2003, 77: 12022–12032.
45. Zhang R, Kim AS, Fox JM, Nair S, Basore K, Klimstra WB, *et al.* Mxra8 is a receptor for multiple arthritogenic alphaviruses. Nature 2018, 557: 570–574.
46. Feng G, Mellor RH, Bernstein M, Keller-Peck C, Nguyen QT, Wallace M, *et al.* Imaging neuronal subsets in transgenic mice expressing multiple spectral variants of GFP. Neuron 2000, 28: 41–51.
47. Guo C, Witter L, Rudolph S, Elliott HL, Ennis KA, Regehr WG. Purkinje cells directly inhibit granule cells in specialized regions of the cerebellar cortex. Neuron 2016, 91: 1330–1341.
48. Witter L, Rudolph S, Pressler RT, Lahlaf SI, Regehr WG. Purkinje cell collaterals enable output signals from the cerebellar cortex to feed back to Purkinje cells and interneurons. Neuron 2016, 91: 312–319.
49. Barski JJ, Dethleffsen K, Meyer M. Cre recombinase expression in cerebellar Purkinje cells. Genesis 2000, 28: 93–98.
50. Zhang XM, Ng AH, Tanner JA, Wu WT, Copeland NG, Jenkins NA, *et al.* Highly restricted expression of Cre recombinase in cerebellar Purkinje cells. Genesis 2004, 40: 45–51.
51. Li M, Liu F, Jiang H, Lee TS, Tang S. Long-term two-photon imaging in awake macaque monkey. Neuron 2017, 93: 1049–1057 e1043.
52. Sawada Y, Kajiwara G, Iizuka A, Takayama K, Shuvaev AN, Koyama C, *et al.* High transgene expression by lentiviral vectors causes maldevelopment of Purkinje cells *in vivo*. Cerebellum 2010, 9: 291–302.
53. Zufferey R, Nagy D, Mandel RJ, Naldini L, Trono D. Multiply attenuated lentiviral vector achieves efficient gene delivery *in vivo*. Nat Biotechnol 1997, 15: 871–875.